



ELSEVIER

Pattern Recognition Letters xxx (2001) xxx-xxx

Pattern Recognition  
Letters

www.elsevier.com/locate/patrec

## Matching of palmprints

Nicolae Duta <sup>a</sup>, Anil K. Jain <sup>b,\*</sup>, Kanti V. Mardia <sup>c</sup>

<sup>a</sup> *Speech and Language Processing Department, BBN Technologies, USA*

<sup>b</sup> *Department of Computer Science and Engineering, Michigan State University, 3115 Engineering Building, East Lansing, MI 48824-1226, USA*

<sup>c</sup> *Department of Statistics, The University of Leeds, UK*

### 8 Abstract

9 This paper investigates the feasibility of person identification based on feature points extracted from palmprint  
10 images. Our approach first extracts a set of feature points along the prominent palm lines (and the associated line  
11 orientation) from a given palmprint image. Next we decide if two palmprints belong to the same hand by computing a  
12 matching score between the corresponding sets of feature points of the two palmprints. The two sets of feature points/  
13 orientations are matched using our previously developed point matching technique which takes into account the non-  
14 linear deformations as well as the outlier points present in the two sets. The estimates of the matching score distri-  
15 butions for the genuine and imposter sets of palm pairs showed that palmprints have a good discrimination power. The  
16 overlap between the genuine and imposter distributions was found to be about 5%. Our preliminary results indicate that  
17 adding palmprint information may improve the identity verification provided by fingerprints in cases where fingerprint  
18 images cannot be properly acquired (e.g., due to dry skin). © 2001 Elsevier Science B.V. All rights reserved.

### 20 1. Introduction

21 Automatic human identification has become an  
22 important issue in today's information and net-  
23 work-based society (Gelsema and Veenland, 1999;  
24 Jain et al., 1999). The techniques for automatically  
25 identifying an individual based on his physical or  
26 behavioral characteristics are called biometrics.  
27 Biometric systems are already employed in a va-

riety of domains that require some sort of user  
verification (e.g., for access control or welfare  
disbursement programs). Numerous distinguishing  
traits that have been used for personal identifica-  
tion include fingerprints, palmprints, face, voice,  
iris and hand geometry. It is generally accepted  
that fingerprint and iris patterns can uniquely de-  
fine each member of an extremely large population  
which makes them suitable for large-scale recog-  
nition (establishing a subject's identity). However,  
in many applications, we only need to authenticate  
a person (confirm or deny the person's claimed  
identity). In these situations, one can also use  
different biometric traits such as voice, hand shape  
or palmprint.

\* Corresponding author. Tel.: +1-517-353-6484; fax: +1-517-432-1061.

E-mail addresses: dutanico@bbn.com; http://web.cse.msu.edu/~dutanico (N. Duta), jain@cse.msu.edu; http://web.cse.msu.edu/~jain (A.K. Jain), k.v.mardia@leeds.ac.uk; http://www.amsta.leeds.ac.uk/~sta6kvm (K.V. Mardia).

43 The science of fingerprints for identification is  
44 well established (Lee and Gaensslen, 1994). The  
45 work was pioneered by Galton (1892) who based  
46 his research on Herschel's data (Cherill, 1954).  
47 Herschel also kept a record of handprints at in-  
48 tervals ranging over long periods which were used  
49 to test the persistence of the ridge characteristics.  
50 Henry's classification was used in classifying fin-  
51 gerprints (Cherill, 1954) but for hand prints only a  
52 few systems have been advanced (Zhang and Shu,  
53 1999; Alexander, 1973; Wilder and Wentworth,

1918). To our knowledge, none of these have been  
54 adopted in practice. While geometry of hands has  
55 been used in biometrics or identity verification,  
56 such systems are not very robust (Jain and Duta,  
57 1999). Dermatoglyphics is another scientific area  
58 where palm patterns (ridge patterns, creases) are  
59 used to correlate them with medical disorders, e.g.,  
60 genetic disorders and Downs syndrome. 61

This paper investigates to what extent the  
62 identity of a person can be verified based on fea-  
63 ture points extracted from palmprints. Adding 64

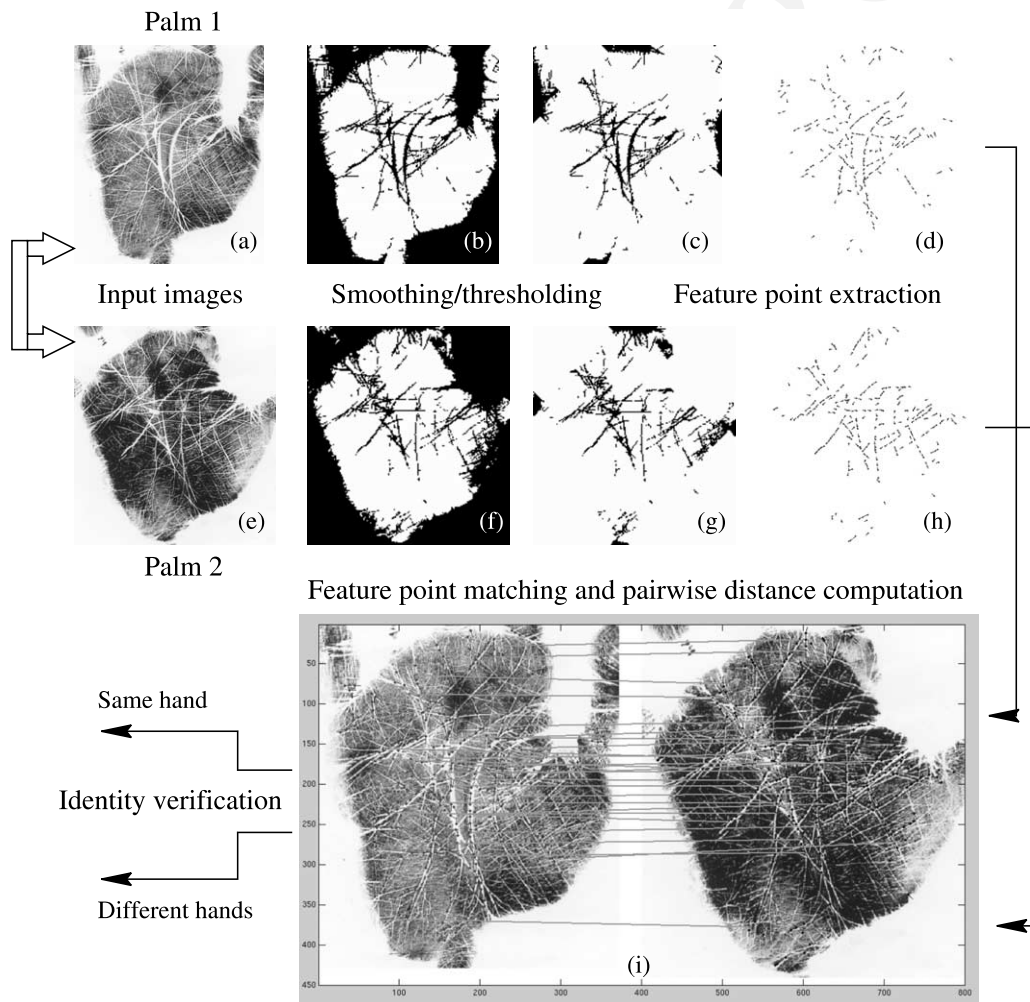


Fig. 1. Palmprint-based identity verification system: (a), (e) Original gray scale image of palms. (b), (f) Binarized palm images. (c), (g) Palm line pixels resulting from (b), (f) after morphological transformations. (d), (h) About 300 feature points/orientations computed by subsampling the feature points in (c), (g) along with their corresponding line orientation. (i) 25 out of the 153 point correspondences found between the feature points in (d) and (h). The matching score is (54%, 4.73).

65 palmprint information may improve the discrimi-  
66 nation provided by fingerprints in cases where  
67 fingerprint information cannot be properly col-  
68 lected (a person's fingerprint may exhibit cuts or,  
69 sometimes, it may be even missing) (Jain et al.,  
70 1999).

## 71 2. Proposed method

72 Given a pair of palmprints, we propose the  
73 following palm matching paradigm (see also Fig.  
74 1):

1. *Feature point extraction.* We define as feature 75  
76 points those points lying on the prominent palm  
77 lines. However, we do not explicitly extract palm  
78 lines as in (Zhang and Shu, 1999), but use only  
79 isolated points that lie along palm lines. We believe  
80 this is a faster way to extract features and that the  
81 feature point connectivity is not essential for  
82 matching purposes. For each such feature point,  
83 the orientation of its associated palm line is also  
84 computed. The feature points were extracted as  
85 follows:

- (i) The palm image is smoothed by replacing 86  
87 each pixel value with the average of its original  
88 value and the values of its four immediate



Fig. 2. Feature point matchings (both point positions and orientations are matched) corresponding to the palmprint pair in Fig. 1(i). The 153 point correspondences found are shown using light gray segments. The six main palm lines which have been matched are shown inside the solid gray areas. Due to a different position of the thumb in the two palm scans, the diagonal palm lines inside the ellipsoidal area differ by a non-linear transformation.

89 neighbors. Smoothing is aimed at removing local  
90 noise and very thin palm lines (the prominent  
91 palm lines are 6–10 pixels wide).

92 (ii) The smoothed image is binarized by applying  
93 an interactively chosen threshold  $T$ . All pixels  
94 whose values are greater than  $T$  are regarded  
95 as palm line pixels while the remaining ones are  
96 considered to be part of the background (Fig.  
97 1(b), (f)).

98 (iii) A set of successive morphological erosions,  
99 dilations and subtractions are performed in order  
100 to remove the compact regions misclassified as  
101 palm lines (Fig. 1(c), (g)). The remaining  
102 foreground pixel locations are subsampled in  
103 order to obtain a set of 200–400 pixel locations  
104 which will be considered to be the feature points  
105 (Fig. 1(d), (h)).

106 (iv) Each feature point location is adjusted to be  
107 the pixel of maximum average gray value in a  
108  $4 \times 4$  neighborhood of its original location. This  
109 operation is an attempt to place the feature  
110 points along the medial axis (which is approxi-  
111 mated by the set of maximum pixel values along  
112 a palm line) of its corresponding palm line.

113 (v) For each feature point, the orientation of its  
114 corresponding palm line is computed as the di-  
115 rection of the line segment of length 8 which  
116 has the maximum average contrast (absolute  
117 difference value) to its immediate surrounding  
118 (parallel segments placed 2 pixels above and be-  
119 low the given segment).

120 (vi) Since spurious feature points are still pre-  
121 sent, those points whose contrast (defined in  
122 step (v) above) is among the lowest 30% of all  
123 feature points are removed.

124 2. *Pairwise distance computation.* The two sets  
125 of feature points/orientations are matched (as ex-  
126 plained in Section 3) and a matching score is  
127 computed. We define the matching score as a tuple  
128  $(P, D)$ , where  $P$  is the percentage of point corre-  
129 spondences with respect to the minimum number  
130 of feature points in the two sets, and  $D$  is the av-  
131 erage distance (in pixels) between the correspond-  
132 ing points. The choice for this matching score was  
133 motivated by the two sources of variation present  
134 in different palm images of the same subject: (i)  
135 noise introduced by feature point extraction and

(ii) non-linear palm deformations due to various  
136 finger positions. 137

The  $P$  component of the matching score at-  
138 tempts to model the amount of noise present in the  
139 feature point set. Consider for example that  $S$  is  
140 the set of “true” feature points along the main  
141 palm lines in Fig. 1(a). Due to image noise and  
142 limitations of the feature extraction procedure, we  
143 can only compute an estimate  $\hat{S}$  of  $S$  which is the  
144 set of feature points actually shown in Fig. 1(d).  
145 Some of the “true” feature points could not be  
146 detected, while several spurious points were in-  
147 troduced. If we assume that only 80% of the points  
148 in  $S$  could be retrieved in  $\hat{S}$  and the remaining  
149 points in  $\hat{S}$  represent independent noise which are  
150 less likely to have matching points in a different  
151 instance of the same palm, then we might expect to  
152 find about  $80\% \times 80\% = 64\%$  (with respect to the  
153 number of “true” feature points in  $S$ ) point cor-  
154 respondences between two instances of the same  
155 palm. The  $D$  component of the matching score  
156 models the amount of non-linear deformation  
157 between two instances of the same palm. This is  
158 shown in Fig. 2 where, due to a different position  
159 of the thumb, the main diagonal palm line is  
160 somewhat rotated between the two images. Since  
161 the point matching only takes into account simi-  
162 larity transformations (composition of translation,  
163 rotation and scaling), non-linear deformations will  
164 increase the average distance between the corre-  
165 sponding points. Our approach does not attempt  
166 to model natural palm variations present in dif-  
167 ferent subjects. This is a difficult task, and for  
168 palmprints, we do not believe that the three types  
169 of variation present (natural, noise and non-linear  
170 deformation) could be easily modeled separately. 171

3. *Identity verification.* Once the matching tuple  
172  $(P, D)$  between two palmprints has been com-  
173 puted, the identity verification becomes a two-class  
174 (genuine vs. imposter) classification problem. The  
175 classification task can be treated as constructing a  
176 decision boundary in a  $2D$  feature space ( $P$  and  
177  $D$  are treated as two features), or some projection  
178 method can be applied in order to transform the  
179 data into a one-dimensional feature space. We  
180 chose to apply a discriminant analysis to the sets of  
181 intra-class and inter-class (genuine/imposter)  
182 matching scores in order to obtain a one-dimen-  
183

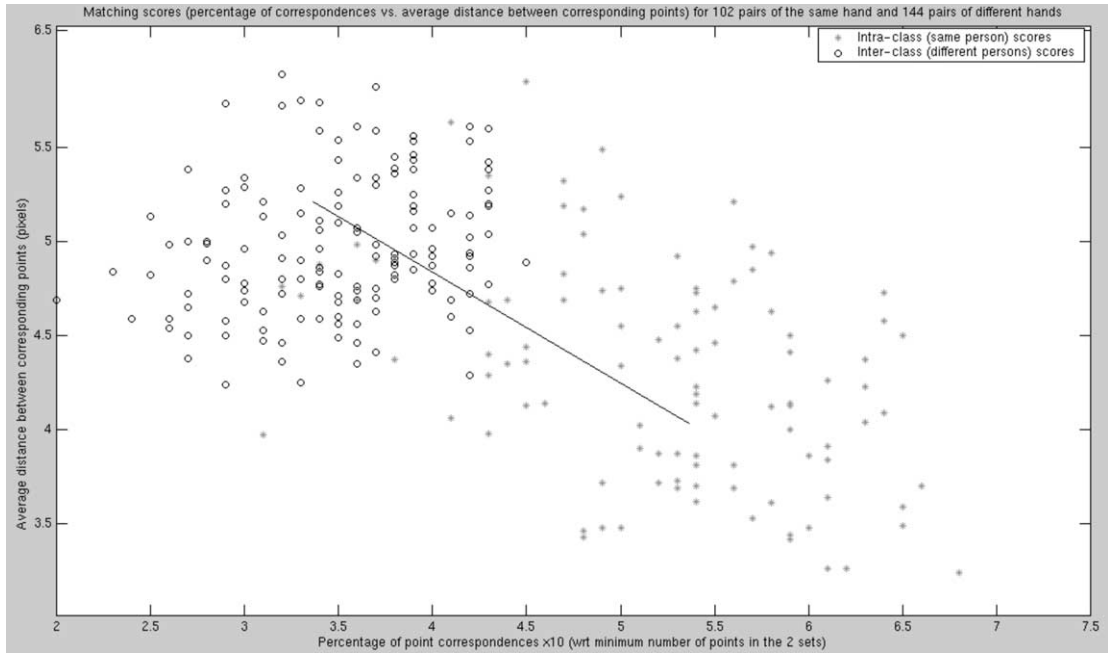


Fig. 3. Matching score tuples (percentage of correspondences vs. average distance between corresponding points) for the 102 intra-class pairs and 144 inter-class pairs. The line segment is the most discriminant axis (the projections of the points onto this line are most separable).

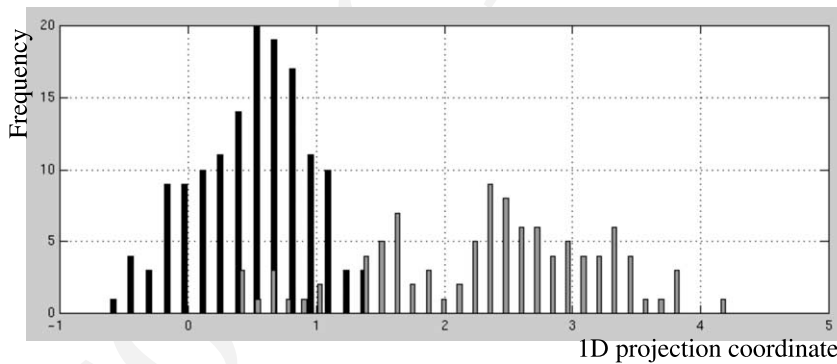


Fig. 4. Histograms of the 2D point projections on the most discriminant axis in Fig. 3. There is about 94% discrimination between the genuine and imposter distributions.

184 sional “similarity” score for the two palmprints  
185 (see Fig. 3). In this way, the decision rule reduces  
186 to a simple thresholding and the Neymann–Pearson  
187 rule that minimizes the false reject rate (FRR)  
188 for a fixed false accept rate (FAR) is employed to  
189 compute the “optimum” threshold (see Fig. 4).

### 3. Feature point matching

190

As mentioned in Section 2, we represent the  
features of a palmprint by a set of points in the  
Euclidean plane along with the palm line orientation  
at each feature point. Feature point matching

191  
192  
193  
194

195 is the process of geometrically aligning two or  
196 more sets of points derived from images of the  
197 same object. Most studies dealing with point  
198 matching generally agree that if  $D$  is a “distance”  
199 function between two sets of points  $A$  and  $B$ , then  
200 the point set  $B$  is *aligned* to the point set  $A$  with  
201 respect to a transformation group  $G$  (e.g., rigid,  
202 similarity, linear, affine) if  $D(A, B)$  cannot be de-  
203 creased by applying to  $B$  a transformation from  $G$ .  
204 We use a least-squares type distance because there  
205 exists an analytical (exact) solution to the align-  
206 ment problem once the point correspondences are  
207 known (Dryden and Mardia, 1998). However, in  
208 order to use a least-squares alignment method one  
209 should find point correspondences between the  
210 two sets. Most of the time, the point sets are au-  
211 tomatically derived from images, so there are no  
212 known correspondences between them. Moreover,  
213 some points may have no correspondence so they  
214 should be rejected as outliers.

215 We have developed a registration procedure  
216 (Duta et al., 2001) based on a polynomial quasi-  
217 exhaustive exploration of the correspondence  
218 functions (match matrices) space. Its main novelty  
219 compared to techniques previously used in the  
220 literature (Besl and McKay, 1992; Gold et al.,  
221 1998; Feldmar and Ayache, 1996; Bookstein, 1997)  
222 is the way it resolves the *shrinking* effect (Feldmar  
223 and Ayache, 1996): an unconstrained linear regis-  
224 tration of two sets of points tends to “shrink” one  
225 set with respect to the other since, theoretically,  
226 the “best” alignment is obtained when one point  
227 set is rescaled to become a single point. Our  
228 problem formulation requires a small *mean align-*  
229 *ment error*<sup>1</sup> between the two chosen subsets, using  
230 as many point correspondences as possible. Un-  
231 fortunately, if we have less than three correspon-  
232 dences, the MAE is 0 and this should be  
233 compensated for. Therefore, we want to explicitly  
234 specify in the search criterion that a  $q\%$  increase in

MAE with a  $p\%$  increase in the number of corre- 235  
spondences is accepted as long as no individual 236  
distance between a pair of corresponding points 237  
exceeds a given threshold. One of the simplest 238  
functionals that captures this trade-off is the ratio 239  
between a compensated MAE and the number of 240  
correspondences: 241

$$f(M) = [\text{MAE}(M) + K]/n, \quad (1)$$

where  $K$  is a constant depending on the percent- 243  
ages  $p$ ,  $q$  and the scale of the object (see (Duta et 244  
al., 2001) for the properties of this functional and 245  
how to choose  $K$ ). If we also impose the constraint 246  
that the mapping is one-to-one, we implicitly solve 247  
the shrinking problem. With a large number of 248  
one-to-one correspondences (and the assumption 249  
that the two shapes are not sampled at very dif- 250  
ferent rates), there can be no shrinking of one 251  
shape with respect to the other. We denote by  $A$  252  
and  $B$  the two sets of feature points to be matched. 253  
Following is a high level description of our regis- 254  
tration algorithm. 255

1. Set  $V_{\min} = \infty$ . 256
2. For every pair of points  $(a_{j1}, a_{j2}) \in A \times A$  257
  - For every pair of points  $(b_{k1}, b_{k2}) \in B \times B$ , do 258
    - steps (i)–(v) 259
    - (i) Find the similarity transformation  $\psi$  that 260  
aligns the sets  $\{a_{j1}, a_{j2}\}$  and  $\{b_{k1}, b_{k2}\}$ . 261
    - (ii) Apply  $\psi$  to all the points in  $B$  to obtain  $B'$ . 262
    - (iii) For every point  $b_k$  of  $B'$ , find its nearest 263  
neighbor  $\text{NN}(b_k)$  in  $A$ . If the distance be- 264  
tween  $b_k$  and  $\text{NN}(b_k)$  is smaller than a thresh- 265  
old  $T$  and the associated line orientations do 266  
not differ by more than  $45^\circ$  then set a corre- 267  
spondence between the two points. A match 268  
matrix  $M$  between  $A$  and  $B$  is constructed 269  
in this way. Since two points from  $B'$  can 270  
have the same nearest neighbor in  $A$ , we en- 271  
force the one-to-one correspondence require- 272  
ment, that is, allow a point to be linked to its 273  
second to fifth nearest neighbor if the first 274  
one can be assigned to a closer point in  $B'$ , 275  
and the length of the link does not exceed 276  
 $T$ . Recompute the transformation  $\psi$  that 277  
aligns the sets  $A$  and  $B$  according to the 278  
match matrix  $M$ . 279
    - (iv) Compute  $f(M)$ . 280
    - (v) If  $f(M) < V_{\min}$  then  $V_{\min} = f(M)$ ,  $\psi_{\min} = \psi$ . 281

<sup>1</sup> An  $n$ -point set  $B = \{(x_i^B, y_i^B)\}_{i=1, \dots, n}$  is said to be *aligned* to  $A = \{(x_i^A, y_i^A)\}_{i=1, \dots, n}$  if the *sum-of-squares*  $\text{SS}(A, B) = \sum_{i=1}^n [(x_i^A - x_i^B)^2 + (y_i^A - y_i^B)^2]$  cannot be decreased by scaling, rotating or translating  $B$ . In this case,  $\text{SS}(A, B)$  is called *Procrustes distance* between  $A$  and  $B$  (Dryden and Mardia, 1998), and the ratio  $\text{SS}(A, B)/n$  is called the *mean alignment error* ( $\text{MAE}(A, B)$ ).

- 282 3. Apply  $\psi_{\min}$  to all the points in  $B$  to obtain  $B'$ .  
283 4. For every point  $b_k$  of  $B'$ , find its nearest neighbor  
284 in  $A$ . If the distance between  $b_k$  and its nearest  
285 neighbor is smaller than  $T$  and the  
286 associated line orientations do not differ by  
287 more than  $45^\circ$  then set a correspondence between  
288 the two. A match matrix  $M'$  between  $A$   
289 and  $B$  is constructed in this way and enforced  
290 to correspond to one-to-one links.  
291 5. Find the linear transformation  $\psi_{\text{final}}$  that aligns  
292 the corresponding sets  $A_{M'}$  and  $B_{M'}$ .

#### 293 4. Experimental results and discussion

294 A small data set of 30 (15 of each of the two  
295 hands) palmprint images of three persons was  
296 collected (12 prints of each of two persons, and 6  
297 prints of the third one). There are various methods  
298 available to take palmprints as recently summarized  
299 by Reed and Meier (1990). However, since  
300 we wanted to study palmprints under different  
301 stretchings of palm, these methods did not seem to  
302 be suitable. The method for hand prints which we  
303 use depends on a specially designed handprint box  
304 which allows for differing hollowness of palm.  
305 Namely, the box contains a tough rubber pad  
306 framed on the top of which the subject's hand is  
307 placed but the rubber is elastic enough for the  
308 hand of the person taking the print to be placed  
309 inside and pressed firmly against the rubber, ensuring  
310 that the whole of the subject's handprint is clearly  
311 printed. The paper palmprints were scanned using  
312 a Hewlett Packard ScanJet 5200 flatbed scanner at  
313 a resolution of 200 dpi (image size  $400 \times 300$   
314 with 256 gray levels). The entire palm was preserved;  
315 fingers and thumb were omitted. Since no electronic  
316 sensors were used for the palmprint acquisition,  
317 the impression quality varied; some prints were very  
318 homogeneous while others missed the central palm  
319 region as well as other details. The data were  
320 acquired in two sessions separated by a week and  
321 three different finger positions for each hand were  
322 used per session.  
323 From each palmprint, a set of approximately  
324 300 feature points was extracted according to the  
325 algorithm presented in Section 2. Subsequently,  
326 for almost each palm pair that could be formed

327 from the available data (a few pairs were omitted  
328 due to poor palm image quality) a matching score  
329 tuple was computed. As such, the density of the  
330 intra-class (respectively, inter-class) scores was  
331 estimated from 102 intra-class (respectively, 144)  
332 pairs. We show the alignment of a palmprint pair  
333 belonging to the same hand in Figs. 1(i) and 2 (for  
334 a detailed set of alignment results see <http://web.cse.msu.edu/~dutanico>). The different  
335 positions of the thumb in the two palmprints introduced  
336 non-linear deformations in the line structure  
337 (see the relative positions of the diagonal lines inside  
338 the ellipsoidal gray area in Fig. 2). For this  
339 reason, the average distance between the corresponding  
340 points associated with this palm pair (4.73) is larger  
341 than the average.  
342

343 The resulting matching score tuples are plotted  
344 in Fig. 3; the intra-class (genuine) scores are denoted  
345 by “\*” while the inter-class (imposter) scores are  
346 denoted by “o”. One can notice that the genuine  
347 distribution resembles a 2D Gaussian centered at  
348 about 55% point correspondences and about 4 pixel  
349 distance between the corresponding points. This  
350 corresponds to about 25–30% independent noise in  
351 each feature point set as discussed in Section 2.  
352 The orientation of the ellipsoidal cloud is probably  
353 due to non-linear deformations, otherwise the average  
354 distance should not increase when the number of  
355 correspondences decreases. Also, the intra-class  
356 matching scores do not seem to depend on which  
357 hand pair (both left hands or both right hands) is  
358 matched. This shows that the two sources of variation  
359 discussed in Section 2 (noise and non-linear  
360 deformations) act consistently over the entire set  
361 of genuine palm pairs. However, the percentage of  
362 point correspondences between two palmprints is  
363 determined by the quality of the palm scan; for  
364 poor quality scans the “\*” cloud in Fig. 3 is  
365 shifted to the left.

366 The inter-class (imposter) distribution also  
367 resembles a 2D Gaussian centered at about 35%  
368 point correspondences and about 5 pixel difference  
369 between the corresponding points. The orientation  
370 of the cloud is almost perpendicular to that of the  
371 genuine distribution cloud. This type of dependency  
372 between the percentage of point correspondences  
373 and the average distance between corresponding  
374 points is mostly encountered when

375 matching two sets of random points: the larger the  
 376 number of point correspondences, the greater is  
 377 the distance between the corresponding points,  
 378 denoting that there is no clear good match between  
 379 the two sets. The overlap between the genuine and  
 380 the imposter distributions (the “\*” points inside  
 381 the “o” cloud) is primarily due to poor quality  
 382 images in which the percentage of noise is about  
 383 40%.

384 The direction which best discriminates the  
 385 genuine distribution from the imposter distribu-  
 386 tion is shown in Fig. 3 and is roughly parallel to  
 387 the main axis of the genuine distribution. By  
 388 projecting all 2D points onto this axis, one obtains  
 389 the two 1D distributions shown in Fig. 4. One can  
 390 notice that in this case discriminant analysis has  
 391 almost the same discrimination power as the  
 392 quadratic decision boundary applied to the origi-  
 393 nal 2D data. By setting the decision boundary  
 394 (threshold) at 1.25 there are 14 (12 genuine and 2  
 395 imposter) palm pairs which are misclassified. This  
 396 corresponds to a  $14/246 = 5.7\%$  total error rate.

397 Finally, we would like to mention that the point  
 398 matching method described in Section 2 is not it-  
 399 erative (compared to previous methods as in  
 400 (Bookstein, 1997)), that is, Step 2(iii) in our  
 401 matching algorithm does not use a convergence  
 402 criterion. Of course, if we perform Step 2(iii) sev-  
 403 eral times, the resulting match matrix may be  
 404 slightly different (up to about 5% of the feature  
 405 points may have a different corresponding feature  
 406 point or may be rejected as outliers). This is mostly  
 407 due to thresholding the distance between corre-  
 408 sponding points (e.g., a very small rotation of one  
 409 point set can make the distance between several  
 410 pairs of corresponding points exceed the threshold  
 411  $T$  and, as such, these points will be considered  
 412 outliers by the new match matrix). The thresh-  
 413 holding also makes our point matching method  
 414 asymmetric (the final match matrix when matching  
 415 a point set  $A$  to a point set  $B$  may be slightly dif-  
 416 ferent than the one obtained when matching  $B$  to  
 417  $A$ ). However, since we use a large number of fea-  
 418 ture points, the influence of the asymmetry on the  
 419 final  $(P, D)$  matching tuple is small (the estima-  
 420 tions of the genuine and imposter distributions in  
 421 Fig. 3 were computed based on ordered palm pairs

and matching score asymmetry was within 5% and 422  
 seemed to be random). 423

**5. Conclusions 424**

We have presented a preliminary study of a 425  
 palmprint-based method for personal identity 426  
 verification. Our approach first extracts a set of 427  
 feature points along the main palm lines (and the 428  
 associated line orientation) from each palmprint. 429  
 Next we decide if two palmprints belong to the 430  
 same hand by classifying the scores resulting from 431  
 matching the feature sets of the two palmprints. 432  
 The estimation of the matching score distributions 433  
 for the genuine and imposter sets of palm pairs 434  
 showed that palmprints have a good discrimina- 435  
 tion power. The overlap between the genuine and 436  
 imposter distributions was found to be about 5%. 437  
 However, these results may be biased by the small 438  
 size of the data set which we have used. In this 439  
 study the overlap is due exclusively to the noise 440  
 present in the palm images or other non-linear 441  
 deformation, but if more subjects are added, one 442  
 should expect some overlap due to similar palms 443  
 of different persons. To investigate this matter 444  
 further, we plan to collect additional data and to 445  
 re-estimate the genuine and imposter distributions. 446

**References 447**

Alexander, H.V., 1973. *Classifying Palm Prints*. Charles C. 448  
 Thomas, Illinois. 449  
 Besl, P., McKay, N., 1992. A method for registration of 3-D 450  
 shapes. *IEEE Trans. Pattern Anal. Machine Intell.* 14 (2), 451  
 239–256. 452  
 Bookstein, F.L., 1997. Landmark methods for forms without 453  
 landmarks: morphometrics of group differences in outline 454  
 shape. *Med. Image Anal.* 1 (3), 225–244. 455  
 Cherill, F.R., 1954. *The Fingerprint System at Scotland Yard*. 456  
 Her Majesty’s Stationary Office, London. 457  
 Dryden, I.L., Mardia, K.V., 1998. *Statistical Shape Analysis*. 458  
 Wiley, New York. 459  
 Duta, N., Jain, A.K., Jolly, M.P., 2001. Automatic construction 460  
 of 2D shape models. *IEEE Trans. Pattern Anal. Machine* 461  
*Intell.* 23, 1–14. 462  
 Feldmar, J., Ayache, N., 1996. Rigid, affine and locally affine 463  
 registration of free-form surfaces. *Int. J. Comp. Vision* 18, 464  
 99–119. 465  
 Galton, F., 1892. *Finger Prints*. Macmillan, London. 466



- 467 Gelsema, E., Veenland, J., 1999. Pattern recognition in practice. 478  
468 Pattern Recognition Letters 20 (11–13). 479  
469 Gold, S., Rangarajan, A., Lu, C., Pappu, S., Mjolsness, E., 480  
470 1998. New algorithms for 2D and 3D point matching. 481  
471 Pattern Recognition 31 (8), 1019–1031. 482  
472 Jain, A.K., Duta, N., 1999. Deformable matching of hand 483  
473 shapes for user verification. In: Proc. ICIP '99, Kobe, 484  
474 Japan. 485  
475 Jain, A., Bolle, R., Pankanti, S. (Eds.), 1999. Biometrics: 486  
476 Personal Identification in Networked Society. Kluwer 487  
477 Academic Publishers, Boston.
- Lee, H.C., Gaensslen, R.E. (Eds.), 1994. Advances in Finger- 478  
print Technology. CRC Press, Boca Raton. 479  
Reed, T., Meier, R., 1990. In: Taking Dermatoglyphic Prints: 480  
A Self-Instruction Manual. Supplement to the Newsletter 481  
of the American Dermatoglyphics Association, pp. 1–45. 482  
Wilder, H.H., Wentworth, B., 1918. Personal Identification. 483  
The Gorham Press, Boston. 484  
Zhang, D., Shu, W., 1999. Two novel characteristics in 485  
palmprint verification: datum point invariance and line 486  
feature matching. Pattern Recognition 32 (4), 691–702. 487

UNCORRECTED PROOF